Hyperfine Interactions 123/124 (1999) 327–345

Synchrotron radiation time spectra affected by diffusion: theory

V.G. Kohn and G.V. Smirnov

Russian Research Centre "Kurchatov Institute", Moscow 123182, Russia

The general theory and a qualitative picture of time spectra in nuclear resonant scattering of synchrotron radiation in the presence of diffusive motion of atoms are presented. The coherent channel of the nuclear exciton decay with emission of a γ quantum in a primary direction and the incoherent channel are considered. The theory is applied for three cases of diffusive motion: free diffusion in an unrestricted space, diffusion in a limited volume, and jump diffusion in a crystal.

1. Introduction

1.1. Why Mössbauer spectroscopy is suitable for diffusion studies

One of the remarkable properties of nuclear resonant scattering of Mössbauer radiation is the very narrow width of the resonance Γ. Among many applications it offers the possibility of extremely high energy resolution for studying atomic dynamics in condensed matter. For example, the ^{57}Fe nucleus has

$$\Gamma = \begin{cases} 7.07 \cdot 10^6 \text{ s}^{-1} & \text{in frequency scale,} \\ 4.65 \cdot 10^{-9} \text{ eV} & \text{in energy scale,} \\ 0.097 \text{ mms}^{-1} & \text{in velocity scale.} \end{cases} \tag{1.1}$$

The small value of Γ permits the division of the atomic motion processes into processes with high atomic velocities $v \gg \Gamma$ and low atomic velocities $v \approx \Gamma$.

The effects of high and low velocities on nuclear scattering of electromagnetic radiation are very different. Fast spatially unlimited motion destroys coherent resonant scattering completely due to dephasing of the scattered waves (e.g., in gases). Fast motion limited in space (thermal vibrations in liquids and solids) only changes the intensity of coherently scattered radiation by a constant factor. Contrary to thermal vibrations, a diffusive motion often presents low velocities. Frequently the velocity of diffusive motion, v_{d}, is comparable with the width of the nuclear resonance Γ. In this case not only the scattering intensity but the process of scattering itself is influenced by the motion of the nucleus. This brings new features to the energy or time dependence of the scattered intensity. By virtue of this, nuclear resonant scattering gives a unique possibility to probe diffusive atomic motion.

For a long time after the discovery of the Mössbauer effect diffusion was investigated only in the energy spectra of nuclear scattering. The diffusive motion leads to a change of the shape of the Mössbauer spectrum. Recently a powerful technique for studying nuclear γ resonance was developed with the use of nuclear resonant scattering of synchrotron radiation (SR). This technique is based on measuring the time dependence of the radiation re-emitted by nuclei after excitation of the nuclear system by a very short pulse of SR. The observation of coherent re-emission, in particular, into the forward direction, allows us to claim the formation of excitation distributed coherently over the entire nuclear system, called a nuclear exciton, which decays non-exponentially, contrary to the case of individual excited nuclei that exhibit an exponential decay. The diffusion manifests itself in a transformation of the time dependence of the coherent nuclear scattering of SR caused by the spatial re-arrangement of nuclei inside the system during scattering. The well determined direction of the SR beam allows us to study the diffusive motion selectively in different directions. This is of importance for anisotropic diffusion, like that in a cage or in a crystal.

The aim of this section is to examine theoretically the feasibilities and advantages of the coherent nuclear scattering in the time domain to study the diffusive motion of nuclei.

1.2. Diffusion as observed by nuclear time response

The two stages of the process of nuclear resonant scattering, the absorption of a photon and its re-emission, can be well resolved in time with the use of SR. The duration of the synchrotron radiation pulses is much shorter than the nuclear lifetime $\hbar/\Gamma$. Therefore, the short pulse marks the time of the initial excitation of the nuclear ensemble t'. The time of de-excitation of the nuclear ensemble, t, is given by the time of detection of the scattered quantum.

Consider a γ-ray travelling from source to detector in forward scattering. A γ-ray is emitted by a source nucleus at $\mathbf{r}_S$. It is absorbed by a target nucleus at site $\mathbf{r}_\alpha(t')$. Then it is re-emitted by this nucleus from site $\mathbf{r}_\alpha(t)$ and detected at the point $\mathbf{r}_D$ (see figure 1). The total optical path is $\mathbf{k}[\mathbf{r}_\alpha(t') - \mathbf{r}_S] + \mathbf{k}[\mathbf{r}_D - \mathbf{r}_\alpha(t)]$, where $\mathbf{k}$ is the momentum of the photon. The common part of the optical path from source to detector can be omitted, then the phase factor of the scattered γ-ray at the detector is $\exp(-\mathrm{i}\mathbf{k}[\mathbf{r}_\alpha(t) - \mathbf{r}_\alpha(t')])$.

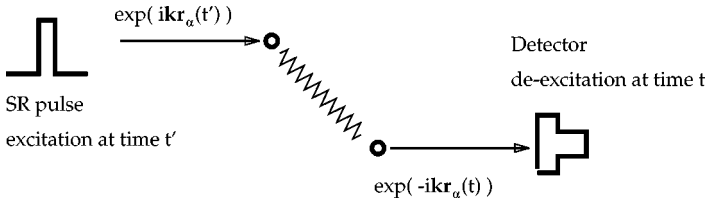

Figure 1. A schematic showing the phase shift during the scattering of photons by nuclei moving diffusively.

If the nucleus is at rest during scattering this factor equals unity. However, if the nucleus changes its position during the scattering process, i.e., in the time interval between the excitation t' and de-excitation t, the phase factor will differ from unity.

As pointed out previously, we can consider two kinds of motion. The fast oscillation (thermal vibration) averages each phase factor, $\exp(\mathrm{i}\mathbf{k}\mathbf{r}_\alpha(t'))$ and $\exp(-\mathrm{i}\mathbf{k}\mathbf{r}_\alpha(t))$, separately. As a result of this averaging only the middle position of the nucleus remains in the phase factor and, in addition, the factor $f_\alpha(\mathbf{k})$ arises in the scattering amplitude, which is the probability of recoilless emission, called the Lamb–Mössbauer factor:

$$\left\langle \exp\left(-\mathrm{i}\mathbf{k}\mathbf{r}_\alpha(t)\right)\right\rangle = f_\alpha(\mathbf{k})\exp\left(-\mathrm{i}\mathbf{k}\bar{\mathbf{r}}_\alpha\right). \tag{1.2}$$

On the other hand, in the case of slow motion (diffusion) we need to consider the whole exponential factor and average it over the total nuclear ensemble because of the collective character of nuclear scattering. This procedure leads to a factor (for more details see [1])

$$F\left(\mathbf{k},t,t'\right) = \frac{1}{N}\sum_\alpha \exp\left(-i\mathbf{k}\left[\mathbf{r}_\alpha(t) - \mathbf{r}_\alpha\left(t'\right)\right]\right), \tag{1.3}$$

where N is the total number of nuclei in the ensemble. The isolated system obeys time homogeneity. Therefore this function depends only on the time difference, namely, $F(\mathbf{k},t,t') \to F_s(\mathbf{k},t-t')$, where

$$F_s(\mathbf{k},t) = \left\langle \exp\left(-\mathrm{i}\mathbf{k}\left[\mathbf{r}(t) - \mathbf{r}(0)\right]\right)\right\rangle \tag{1.4}$$

is a self-correlation function which describes the correlation of the phase factors connected with the same particle at different times. The averaging over an ensemble of particles can be replaced by thermodynamical averaging. This is the function that corresponds to a scattering problem and can be studied in our case by means of nuclear resonant scattering. We will call it the *momentum–time correlation function.*

According to (1.4) the MT correlation function represents the mean value of the phase factor over unit target volume. As a function of time this average phase factor reflects an average diffusive motion of nuclei. The origin of the correlation function is very similar to the Lamb–Mössbauer factor, which describes the damping of the scattering amplitude due to thermal motion. The difference between them is only in the time scales of the motions involved.

The picture described above assumes only single scattering processes, which occur for thin targets. In a thick target multiple scattering processes become essential and the situation becomes more complicated. However, the physical origin of the diffusive motion in nuclear resonant scattering remains the same.

1.3. History and predecessors

The first systematic consideration of the momentum–time correlation function was made by Van Hove [2], who also introduced the space–time self-correlation function

$G_s(\mathbf{r},t)$ which describes the correlation in positions of one and the same particle at different times:

$$G_s(\mathbf{r},t)=\int\frac{\mathrm{d}\mathbf{k}}{(2\pi)^3}\exp(\mathrm{i}\mathbf{k}\mathbf{r})F_s(\mathbf{k},t)=\left\langle\int\mathrm{d}\mathbf{r}'\delta\big(\mathbf{r}+\mathbf{r}(0)-\mathbf{r}'\big)\delta\big(\mathbf{r}'-\mathbf{r}(t)\big)\right\rangle. \quad (1.5)$$

Sometimes the space–time correlation function is more suitable for calculating the correlation itself. Then the momentum–time correlation function can be calculated by means of the inverse Fourier transformation

$$F_s(\mathbf{k},t)=\int\mathrm{d}\mathbf{r}\exp(-\mathrm{i}\mathbf{k}\mathbf{r})G_s(\mathbf{r},t). \quad (1.6)$$

After the discovery of the Mössbauer effect Singwi and Sjölander [3] proposed the theory of nuclear resonance absorption to account for the atomic dynamics.

It was shown that in the presence of diffusive motion the absorption cross-section per nucleus for a γ-ray of frequency ω, with propagation vector $\mathbf{k}$, is given by

$$\sigma(\mathbf{k},\omega)=\frac{\sigma_0\Gamma}{4\hbar}\int\mathrm{d}\mathbf{r}\,\mathrm{d}t\exp\big[-\mathrm{i}(\mathbf{k}\mathbf{r}-\omega t)-\Gamma|t|/2\hbar\big]G_s(\mathbf{r},t). \quad (1.7)$$

This cross-section is tightly related to the universal resonance function (see, for example, [4] and references therein)

$$\varphi(\mathbf{k},\omega)=\int_0^\infty\mathrm{d}t\exp(\mathrm{i}\omega t-\Gamma t/2\hbar)F_s(\mathbf{k},t). \quad (1.8)$$

In fact, only the real part of this function participates in the absorption cross-section. In the last forty years many approaches were developed to calculate this function.

The case of free diffusion was considered by Singwi and Sjölander [3]. Whereas the Singwi–Sjölander theory applies quite generally to atomic diffusion in liquids or solids, Chudley and Elliott [5] and Krivoglaz [6] developed a particular approach, describing diffusion jumps on Bravais lattices containing only one atom in the crystalline unit cell. Rowe et al. [7] have extended the theory to diffusion on non-Bravais lattices.

The first to consider the changes in lineshape due to the hopping of a Mössbauer atom in a restricted space were Krivoglaz and Repetskii [8], who studied theoretically the Mössbauer spectrum of an iron atom bound to and jumping into and around a vacancy. Localized diffusion was analysed for crystalline solids by Petry and Vogl [9] and in biopolymers by Novik et al. [10].

The case of restricted or bounded diffusion can be studied in the frame of the Fokker–Planck equation for the Van Hove space–time self-correlation function. Nadler and Schulton [11] and Afanasev and Sedov [4] developed the regular technique which reduces the problem to usual quantum mechanics but with slightly different boundary conditions. The case of jump diffusion in crystals was intensively studied in papers by Vogl et al. [12].

The result of these investigations can be briefly formulated as follows. In general, the diffusive motion leads to a splitting of the resonance into different components with the same position of the resonance but with different widths. For unrestricted diffusion,

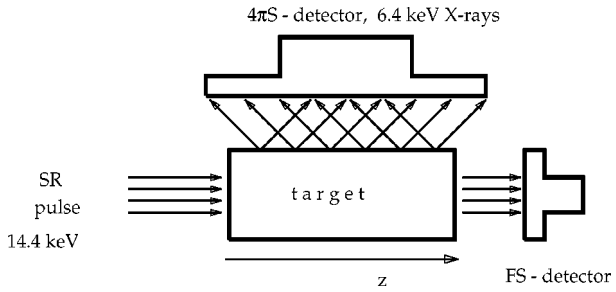

Figure 2. An experimental arrangement for measuring coherent forward scattering and incoherent fluorescence simultaneously.

for example for free diffusion, the nonwidened component has zero weight. However, for motion restricted in space the weight of the nonwidened component is always greater than zero. This weight is determined by the time that the nucleus spends at the central position during its movement.

1.4. What is of interest

First investigations of nuclear resonant scattering of SR were performed with the use of the coherent channel, namely, pure nuclear diffraction of radiation in a single crystal [13]. Pure nuclear diffraction allowed the successful solution of the problem of suppression of nonresonant electronic scattering. Later, the development of high resolution monochromators and the application of fast detectors opened the possibility to work in the more general forward scattering set-up [14]. The coherent forward scattering channel is very suitable for the study of diffusive motion, as shown above. For example, in case of a thin target (in the kinematical scattering approximation) it permits one to measure directly the momentum–time correlation function. Incoherent 4π scattering is also of interest. In the full picture of scattering the balance between forward and 4π scattering becomes more and more in favor of the 4π channel with increasing diffusive motion. Therefore, the incoherent channel becomes especially informative about the presence of intensive diffusive motion. In the case of ^{57}Fe the incoherent channel can be well studied by measuring the secondary fluorescent 6.4 keV quanta from internal conversion (see figure 2). In a thick target the time dependence of the incoherent channel differs from the usual exponential law due to the excitation of nuclei by delayed coherent radiation.

2. Incoherent channel, 6.4 keV fluorescence

The incoherent scattering process is independent for each nucleus. The scattered radiation creates a 4π halo around the target. Such a 4π-scattering involves γ-rays, photoelectrons and X-rays. The time dependence of the X-rays and photo-electrons is the same. However, in the case of ^{57}Fe the 6.4 keV fluorescent X-rays are more

suitable for registration. The detector of the fluorescent radiation collects the quanta which are produced in three scattering processes:

A – internal conversion without recoil,

B – internal conversion with recoil,

C – direct photoelectron emission.

Process A is the most complicated because it is initiated both by incident synchrotron radiation pulses and by delayed coherently scattered radiation (see below). As shown by Smirnov and Kohn [1], the time dependence of this process can be described as

$$I^{\mathrm{A}}_{4\pi}(t,\mathbf{k},d)=\sum_l P_l\int_0^d \mathrm{d}z\int\frac{\mathrm{d}\omega'}{2\pi}F_s\big(\mathbf{k},\omega'\big)\big|D_l\big(t,z,\omega'\big)\big|^2, \tag{2.1}$$

where

$$D_l\big(t,z,\omega'\big)=\int\frac{\mathrm{d}\omega}{2\pi}\exp(-\mathrm{i}\omega t)\frac{E_\omega(z)}{(\omega-\omega'-\omega_l+\mathrm{i}\Gamma/2\hbar)}. \tag{2.2}$$

Here the index l numbers the components of the hyperfine structure of the resonance, P_l is the weight and ω_l is the position of the particular resonance, z is a coordinate inside the sample along the SR beam direction, d is the total thickness of the sample,

$$F_s(\mathbf{k},\omega)=\int \mathrm{d}t\exp(\mathrm{i}\omega t)F_s(\mathbf{k},t) \tag{2.3}$$

is the momentum–frequency correlation function. Finally, $E_\omega(z)$ depends on z, the partial spectral component of the delayed wave field.

The physical meaning of these formulas is the following: the diffusive motion of nuclei leads to a Doppler shift of the resonance. Each shift has a weight just determined by the total space and time Fourier image of the Van Hove self-correlation function (a space–time correlation function in our notation).

The most simple situation arises when there is no diffusion or hyperfine splitting of the nuclear levels. In this case the analytical formula is

$$I^{\mathrm{A}}_{4\pi}(t,\mathbf{k},d)=Cf_{\mathrm{LM}}(\mathbf{k})\exp(-t/t_0)\int_0^d \mathrm{d}z\exp(-\mu_e z)\mathrm{J}_0^2\big(\sqrt{\mu_n z t/t_0}\,\big), \tag{2.4}$$

where

$$C=\frac{I_0}{\Delta\omega}\Gamma_e\Gamma N\sigma_0\eta,\qquad t_0=\frac{\hbar}{\Gamma},\qquad \mu_n=N\sigma_0\eta f_{\mathrm{LM}}(\mathbf{k}), \tag{2.5}$$

J_0 is the zero-order Bessel function, $\Gamma_e=\Gamma/(1+\alpha)$ is the radiation width of the resonance, α is the internal conversion coefficient, N is the number of nuclei per unit volume, σ_0 is the resonance cross-section, η is the enrichment of the resonant isotope ($0<\eta<1$), μ_e is the absorption coefficient outside resonance, μ_n is the nuclear resonance absorption coefficient, $f_{\mathrm{LM}}(\mathbf{k})$ is the Lamb–Mössbauer factor, I_0 is the intensity of SR in the frequency band $\Delta\omega$.

In the case of free diffusion the only broadened resonance has a width $q\Gamma$, where $q = 1 + 2Dk^2/\Gamma$ and D is the diffusion coefficient. In this case an approximate analytical formula can be obtained for small sample thickness and time delay:

$$I^{\mathrm{A}}_{4\pi}(t,\mathbf{k},d) = C f_{\mathrm{LM}}(\mathbf{k}) \int_0^d \mathrm{d}z \exp(-\mu_e z)\big[F(z)\exp(-t/t_0) + G(z,t)\exp(-qt/t_0)\big], \tag{2.6}$$

where

$$F(z) = 1 - h + \cdots, \quad G(z,t) = h - \cdots, \quad h = \frac{\mu_n z}{4Dk^2 t_0} \ll 1, \quad Dk^2 t \ll 1. \tag{2.7}$$

One can clearly distinguish two time dependences in the incoherent scattering. The first, the normal one, is characteristic for free decay of an isolated nucleus. The second is connected with the speeding up of the incoherent scattering induced by the coherent field.

The B-process (internal conversion with recoil) is the incoherent process. It has an obvious time dependence

$$I^{\mathrm{B}}_{4\pi}(t,\mathbf{k},d) = C\big[1 - f_{\mathrm{LM}}(\mathbf{k})\big] \int_0^d \mathrm{d}z \exp(-\mu_e z)\exp(-t/t_0). \tag{2.8}$$

For the C-process (photoelectron emission) the time dependence is determined by that of the forward scattering intensity $I_{\mathrm{FS}}(z,t)$:

$$I^{\mathrm{C}}_{4\pi}(t,d) = N\sigma_{\mathrm{pho}} \int_0^d \mathrm{d}z I_{\mathrm{FS}}(z,t). \tag{2.9}$$

The formulas obtained allow the analysis of different special cases.

3. Coherent channel, forward scattering

The experimental set-up of the transmission geometry is attractive for its simplicity, both for traditional Mössbauer experiments and for those of nuclear resonant scattering of SR. Forward scattering is a coherent process independent of the structure of the target. The diffusive motion of nuclei is a statistically stationary process. Therefore, in propagating through the target a monochromatic wave preserves this property and only its amplitude and phase are changed. Under the condition of time homogeneity the problem can be solved by Fourier transformation, as pointed out by Kagan et al. [15].

Applying the same technique in [1] the formula for the scattered intensity was obtained:

$$I_{\mathrm{FS}}(t,z) = \big|E(t,z)\big|^2,$$

$$E(t,z) = E_0(z) \int \frac{\mathrm{d}\omega}{2\pi} \exp(-\mathrm{i}\omega t) \exp\left(-\frac{\mu_n z}{4t_0} \sum_l P_l \varphi(\mathbf{k}, \omega - \omega_l)\right) \tag{3.1}$$

with $E_0(z)$ from

$$\left|E_0(z)\right|^2 = \frac{I_0}{\Delta\omega}\exp(-\mu_e z). \tag{3.2}$$

Here the notation is the same as in the preceding section and $\varphi(\mathbf{k},\omega)$ is the universal resonance function (see eq. (1.8)). On the other hand, the Mössbauer transmission spectra deal with the energy resolved technique. For a monochromatic wave with a definite photon energy the energy dependent intensity is given by

$$I_{\rm tr}(\omega,z) = \left|E_0(z)\right|^2 \exp\left(-\frac{\mu_n z}{2t_0}\sum_l P_l \mathrm{Re}\left[\varphi(\mathbf{k},\omega-\omega_l)\right]\right). \tag{3.3}$$

As one can see, only the real part of the universal resonance function influences the transmission intensity of Mössbauer transmission spectra while the SR time spectra depend on the total function $\varphi(\mathbf{k},\omega)$. As pointed out in the introduction, for thin targets the following approximate formula holds for the time dependent intensity:

$$I_{\rm FS}(t,z) = C_z\left|F_s(\mathbf{k},t)\right|^2 \exp(-t/t_0)\left|\sum_l P_l \exp(-\mathrm{i}\omega_l t)\right|^2, \tag{3.4}$$

where

$$C_z = \left|E_0(z)\right|^2\left(\frac{\mu_n z}{4t_0}\right)^2, \tag{3.5}$$

and $F_s(\mathbf{k},t)$ is the momentum–time correlation function. *Thus time spectroscopy allows us to measure the momentum–time correlation function directly*.

We note that the analysis of the time behaviour of the nuclear exciton, as the collective excited state of a nuclear ensemble, consists of two steps. At the first step one finds the accurate form of the universal resonance function $\varphi(\mathbf{k},\omega)$. At the second step one performs the analysis of how the shape of the resonance function determines the time behaviour of the nuclear exciton and obtains the SR time spectra. The task of the first step is the same as for finding Mössbauer absorption spectra. We can use the rich experience accumulated in the theory of transmission energy spectra. However, some new aspects may be discovered. Below, we consider in detail some different mechanisms of diffusive motion.

4. Free diffusion in gases and liquids

Free diffusion assumes no restriction on the motion of a nucleus. It is isotropic, quasi-continuous and unlimited in space (see figure 3(a)). It is well known [1,3] that this motion leads to broadening of the resonance. If the hyperfine structure of the nuclear levels is absent, the universal resonance function is

$$\varphi(\mathbf{k},\omega) = \frac{\mathrm{i}}{\omega + \mathrm{i}q/2t_0}, \quad q = 1 + 2Dk^2 t_0, \tag{4.1}$$

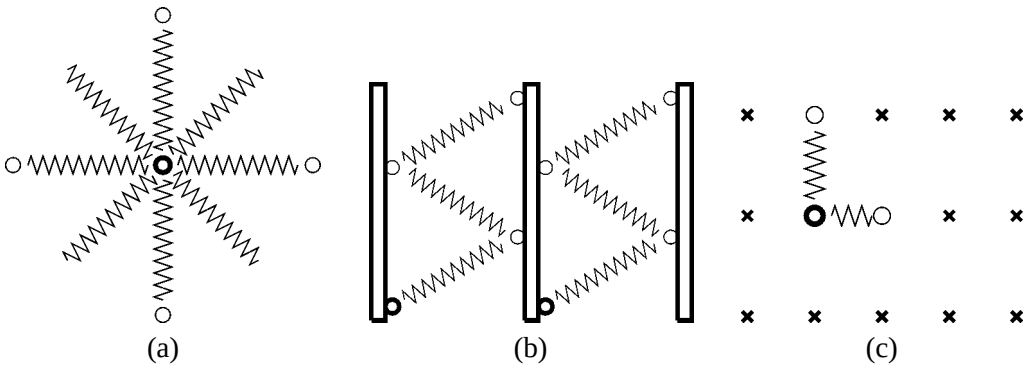

Figure 3. Possible kinds of diffusive motion.

where D is the diffusion coefficient, $t_0 = \hbar/\Gamma$ is the lifetime of the excited state. The momentum–time correlation function in this case is

$$F_s^2(\mathbf{k}, t) = \exp\bigl(-2Dk^2 t\bigr). \tag{4.2}$$

As shown in [1] the analytical solution for the time spectrum is

$$I_{\mathrm{FS}}(t, z) = C_z \exp(-qt/t_0)\frac{4\mathrm{J}_1^2(\sqrt{\mu_n z t/t_0})}{\mu_n z t/t_0}, \tag{4.3}$$

where C_z is determined by eq. (3.5), $\mathrm{J}_1(x)$ is the Bessel function of first order. The case without diffusion corresponds to $q = 1$ in this formula. This result was obtained previously in [15]. From eq. (3.5) one can see that the diffusion influences the time spectrum independent of the effective thickness of target. This means, in particular, that the dynamical beat positions are not sensitive to diffusion.

For small delays $t \ll t_0$ we obtain

$$I_{\mathrm{FS}}(t, z) = C_z \exp(-Qt/t_0), \quad Q = q + \mu_n z/4. \tag{4.4}$$

Since $Q > 1$, one should observe an accelerated decay of the nuclear exciton in the initial stage. As pointed out in [1] there are two reasons for the faster decay of the coherent signal: the coherent speed-up of nuclear de-excitation determined by the target thickness, and accelerated dephasing of the waves contributing to the coherent signal due to diffusive motion. The time-integrated intensity of forward scattering drops due to diffusion.

5. Localized diffusion in gases and liquids

5.1. General theory

Let us call the motion of a nuclear particle spatially restricted under the influence of an external potential localized diffusion. This motion as a rule is limited in space and, dependent on the form of the drift potential, can be quasi-continuous and isotropic.

The general approach is formulated in terms of the Fokker–Planck equation for the Van Hove self-correlation function $G(\mathbf{r}, t)$. However, as shown in [4,11,16], the problem can be reformulated in terms of an effective Schrödinger equation

$$\widehat{H}\psi_n = \varepsilon_n\psi_n, \quad \widehat{H} = D\big[-\nabla^2 + V(\mathbf{r})\big], \quad V(\mathbf{r}) = \frac{(\nabla U(\mathbf{r}))^2}{4T^2} - \frac{\nabla^2 U(\mathbf{r})}{2T}, \tag{5.1}$$

where $U(\mathbf{r})$ is the drift potential of the initial Fokker–Planck equation, D is the diffusion coefficient and T is the temperature in energy units.

The problem in general is reduced to the eigensolution problem for the effective Hamiltonian $\widehat{H}$. The eigenvalues are always positive and they can belong to the discrete spectrum as well as to the continuous spectrum. We will use the index n for both parts of the spectrum. When all eigensolutions of the effective Hamiltonian have been found, the momentum–time correlation function in the absence of hyperfine splitting of nuclear levels can be represented as follows:

$$F_s(\mathbf{k}, t) = \sum_n A_n(\mathbf{k}) \exp(-D\varepsilon_n t) \tag{5.2}$$

with a universal resonance function

$$\varphi(\mathbf{k}, \omega) = \mathrm{i}\sum_n \frac{A_n(\mathbf{k})}{\omega + \mathrm{i}q_n/2t_0}, \quad q_n = 1 + 2D\varepsilon_n t_0. \tag{5.3}$$

As follows from these formulas, a single usual resonance becomes formally split into many resonances with the same energy position but different widths. In fact, it remains a single resonance but of more complicated shape. However, it is convenient to speak about different contributions to the resonance with different widths and weights. The weight of a particular contribution is determined by

$$A_n(\mathbf{k}) = \left| \int \mathrm{d}\mathbf{r} \exp(-\mathrm{i}\mathbf{k}\mathbf{r})\psi_0^*(\mathbf{r})\psi_n(\mathbf{r}) \right|^2, \qquad \sum_n A_n(\mathbf{k}) = 1. \tag{5.4}$$

In accordance with general rules of quantum mechanics the weight is a square modulus of a transition matrix element of the initial state over the diffusion state.

In the case of limited diffusion the initial state $\psi_0^*(\mathbf{r})$ with eigenvalue $\varepsilon_0 = 0$ always has nonzero weight $A_0(\mathbf{k})$. This implies that the unbroadened component of the resonance always exists and its weight is proportional to the average time which the particle spends at a mean position. The case of free diffusion is a particular form of eq. (5.3) with only one component $\varepsilon = k^2$, $A = 1$.

5.2. Bounded diffusion in a cage

The most simple case of limited diffusion is free motion of a particle containing a resonant nucleus inside a cage of definite shape. The drift potential is zero inside and infinity outside the cage. In a spherical cavity of definite radius, such as a hole in a Swiss cheese, this problem was solved by Volino and Dianoux [17]. The

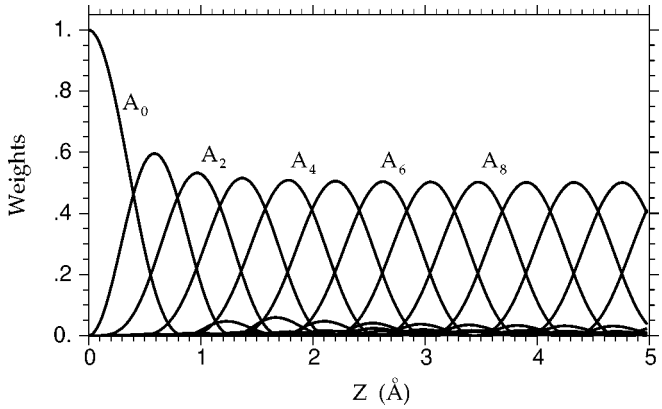

Figure 4. The weights of different components of the resonance function for bounded diffusion.

case of a rectangular cavity is more simple mathematically and it is of interest for understanding the subject. This case can be readily solved using the general theory described above [16]. When the beam propagates along the z-axis, only the z-size of the cage Z is essential. The analytical solution of the eigensolution problem for the effective Hamiltonian can be found. Since the potential has infinitely high walls, only a discrete set of eigenvalues exists. The universal resonance function is described by eq. (5.3) with

$$A_n(k) = \frac{4(kZ)^2}{C_n} \frac{(1+(-1)^{n+1}\cos(kZ)}{((n\pi)^2-(kZ)^2)^2}, \qquad q_n = 1 + 2D\frac{(n\pi)^2}{Z^2}t_0. \tag{5.5}$$

Figure 4 shows the Z-dependence of the weights A_n in the case of ^{57}Fe with $k = 2\pi/\lambda = 7.3$ Å^{-1}. As seen from the figure, the unbroadened Lorentzian dominates only at $Z \ll \lambda$. At each value of Z only two or three Lorentzians have a significant value. However, their indices change with the variation of Z. When Z is large compared to λ only the Lorentzians with index corresponding to the eigenvalues close to the free diffusion case $n\pi/Z \approx k$ are significant.

The Mössbauer absorption spectrum for a thin target looks as a single resonance. The sharpness of the resonance depends on the weight of the component with natural width. Figure 5 shows the absorption spectral function $-\operatorname{Re}\varphi(\mathbf{k},\omega)/2t_0$ for different sizes of the cage Z from 0 to 2 Å with a step of 0.1 Å. For a better view each next curve is shifted upward by 0.05 relative to the previous one. The case of ^{57}Fe and $D = 10^{-14}$ m^{2}s^{-1} is considered. We note that the q-value for free diffusion equals 16 under these conditions.

As for the SR time spectra, they are very different in cases of thin and thick targets. The time dependence for a thin target is described by eq. (3.4), which in this particular case can be written as

$$I_{\mathrm{FS}}(t,z) = C_z f_{\mathrm{FS}}(t,Z), \quad f_{\mathrm{FS}}(t,Z) = \left| \sum_n A_n(k)\exp(-q_n t/t_0) \right|^2. \tag{5.6}$$

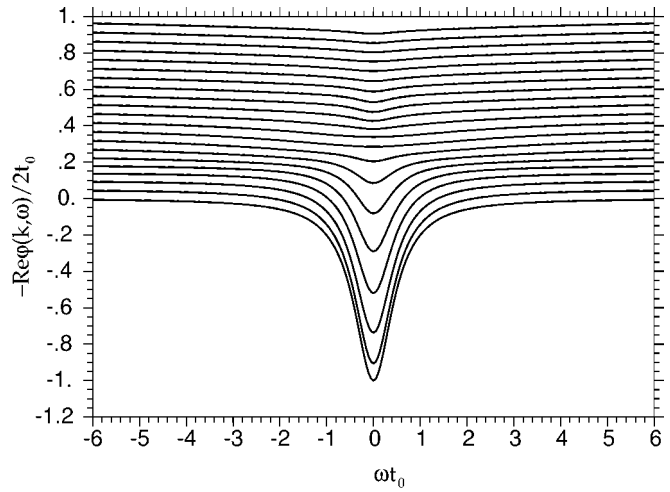

Figure 5. The absorption resonance function for bounded diffusion in a thin target.

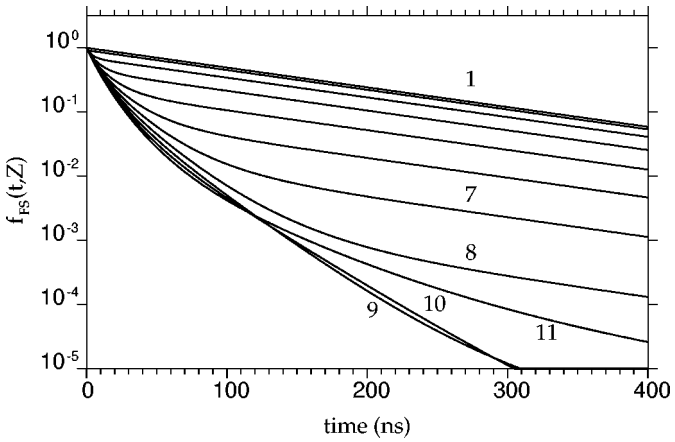

Figure 6. Time spectra of forward scattering for bounded diffusion in a thin target.

The time dependence of relative intensity f_{FS} is shown in figure 6 for different cage sizes Z from 0 to 1 Å with a step of 0.1 Å. Calculations allows us to make the following conclusion. The whole lifetime of the nuclear exciton can be divided into three time domains: an initial domain, an intermediate domain and a steady state domain. Within these domains the time behaviour is different. In the initial domain the nuclear ensemble exhibits free diffusion. The fastest decay occurs inside this domain. It was shown accurately in [16] that *the decay under condition of bounded diffusion cannot be faster than in the case of free diffusion with the same diffusion coefficient*. In the steady state domain the time dependence is determined completely by the natural lifetime of isolated nuclei. However, the intensity can be very low for high Z.

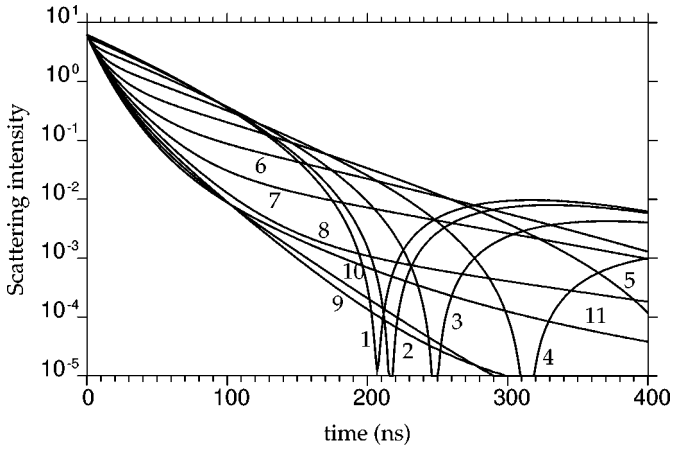

Figure 7. Time spectra of forward scattering for bounded diffusion in a thick target.

The time spectra for thick targets are more complicated. However, they show the same behaviour as in a thin target at a small delay in the initial domain. For a larger time delay, dynamical beats appear similarly to those without diffusion [14,15] or to the case of free diffusion (see section 4). However, contrary to the case of free diffusion, *the positions of the beats are sensitive to the diffusion coefficient and cage size* Z. This sensitivity is clearly seen in figure 7, where the results of calculations are shown for $\mu_n z = 10$ and the other parameters, in particular the cage size Z, are chosen as those in figure 6. The positions of dynamical minima are strongly dependent on the diffusion and cage parameters. Therefore, nuclear resonant scattering of SR can be an effective technique for studying this kind of diffusion. We wish to emphasize one of the merits of this technique: *the long resonance tails reveal themselves in* ***the steepness*** *of the initial slope of the time dependence* which could be obtained from the measurements.

6. Jump diffusion in crystals

The diffusive motion of atoms in crystals at high temperature is anisotropic jumps from one crystal site to the other (see figure 3(c)). This motion in general is unlimited in space but there is a chance that atoms return to the original site after a few jumps. In the case of jumps of atoms on a crystalline lattice the Fokker–Planck equation is not valid. However, as shown in [12] the problem can again be reduced to finding the eigensolution of the Hermitian probability jump matrix, which can be written as follows:

$$G_{ij}(\mathbf{k}) = \frac{2t_0}{\sqrt{c_i}}\left(\delta_{ij}\sum_q \frac{1}{\tau_{iq}} - \frac{1}{n_{ji}\tau_{ji}}\sum_n \exp\left(\mathrm{i}\mathbf{k}\mathbf{R}_{ij}^{(n)}\right)\right)\sqrt{c_j}, \tag{6.1}$$

where c_i is the probability of occupation of the ith sublattice, n_{ji} is the number of sites of the ith sublattice which surround the site of the jth sublattice, $1/\tau_{ij}$ is the jump

rate from the site of symmetry i to any nearest-neighbour site of symmetry j, $\mathbf{R}_{ij}^{(n)}$ is the nth vector-distance of the set of distances between nearest-neighbour sites of the ith and jth sublattices. In the approximation, when only the jumps to nearest neighbouring sites are taken into account, the rank of the jump matrix is not large and only few states are possible.

If the eigenvalues ε_n and eigenvectors β_n of this matrix are found one can write the momentum–time correlation function directly:

$$F_s(\mathbf{k},t) = \sum_n A_n(\mathbf{k}) \exp\bigl(-\varepsilon_n(\mathbf{k})t/2t_0\bigr), \tag{6.2}$$

where

$$A_n(\mathbf{k}) = \left| \sum_{i=1}^{m} \sqrt{c_i}\beta_{in} \right|^2, \qquad \sum_n A_n(\mathbf{k}) = 1. \tag{6.3}$$

The universal resonance function can be written similarly:

$$\varphi(\mathbf{k},\omega) = \mathrm{i} \sum_n \frac{A_n(\mathbf{k})}{\omega + \mathrm{i}q_n(\mathbf{k})/2t_0}, \qquad q_n(k) = 1 + \varepsilon_n(\mathbf{k}). \tag{6.4}$$

In each particular case the time spectrum will depend on parameters like crystal structure and jump rates in different sites. The general theory described above allows a detailed analysis of each particular situation. It is beyond the scope of this paper to discuss all possible situations. Instead, we consider only one particular case, which was investigated in the first study of diffusion with the use of SR [18,19], namely, the forward nuclear scattering of SR along the [1 1 3] crystal direction in Fe_3Si. Single crystals of Fe_3Si have a cubic superstructure with four sublattices. In the entirely ordered crystal the three sublattices are occupied by Fe atoms. The Fe atoms jump between three iron sublattices only and avoid the silicon sublattice.

In this particular case the jump matrix can be written as

$$G = \begin{pmatrix} 2\nu & -E\nu & -E^*\nu \\ -E^*\nu & \nu & 0 \\ -E\nu & 0 & \nu \end{pmatrix}, \quad \nu = \frac{2t_0}{\tau}, \tag{6.5}$$

where τ is the time between jumps and

$$E = \cos(k_x d)\cos(k_y d)\cos(k_z d) + \mathrm{i}\sin(k_x d)\sin(k_y d)\sin(k_z d) \tag{6.6}$$

and $d = a/4$, $a = 5.71$ Å is the lattice constant. Since the matrix is of third rank three eigensolutions are possible. However, in some specific directions one or two Lorentzians may have zero weight. It turned out that for the [1 1 3] direction $k_x d =$

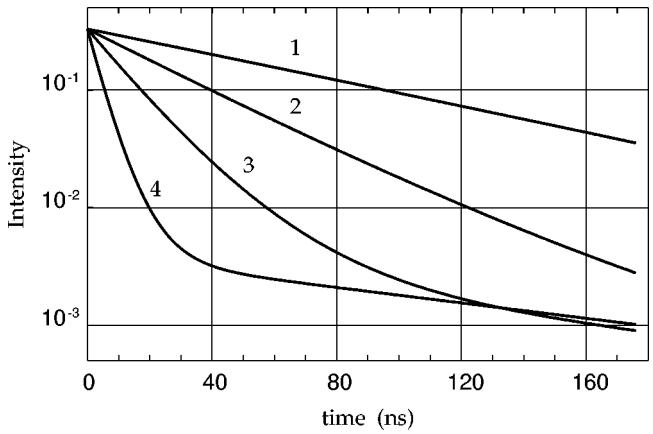

Figure 8. Time spectra of forward scattering for jump diffusion in a thin target.

$k_y d = 3.1411 \approx \pi$, $k_z d \approx 3\pi$. Therefore, to a very good approximation $E = E^* = -1$ and the jump matrix has the following analytical solution:

$$\begin{aligned} \varepsilon_n &= \quad 3\nu \qquad\qquad \nu \qquad\qquad 0 \\ \beta_n &= \frac{1}{\sqrt{6}}\begin{pmatrix}2\\1\\1\end{pmatrix} \quad \frac{1}{\sqrt{2}}\begin{pmatrix}0\\1\\-1\end{pmatrix} \quad \frac{1}{\sqrt{3}}\begin{pmatrix}-1\\1\\1\end{pmatrix} \\ A_n &= \quad 8/9 \qquad\qquad 0 \qquad\qquad 1/9 \end{aligned} \tag{6.7}$$

Correspondingly the universal resonance function is described by two Lorentzians and depends only on one parameter q, namely,

$$\varphi(\mathbf{k},\omega) = \frac{\mathrm{i}}{9}\left(\frac{8}{\omega + \mathrm{i}q/2t_0} + \frac{1}{\omega + \mathrm{i}/2t_0}\right). \tag{6.8}$$

The time spectrum is calculated in accordance with the general formulas eq. (3.1). We will disscuss once again the cases of thin target (figure 8) and thick target (figure 9). Figure 8 shows the time dependence of the forward scattered intensity for $\mu_n z = 3$ and $q = 2.2, 5.1, 11.5$ and 36, corresponding to curves 1–4 (to single out the diffusion effect the Lamb–Mössbauer factor was artificially assumed to be constant in the temperature region under study).

In the thin target limit, using eq. (6.8) and approximation equation (3.4), one can readily find that the MT correlation function is described by the sum of two exponentials, one of which exhibits the natural decay of the nuclear excitation while the other shows the accelerated decay. With the increase of the q-factor, the acceleration of the decay is well seen within the initial time interval in figure 8. In the limit $q \gg 1$, the two exponential functions turn out to be well separated in time and the two stages of the decay are clearly observed.

The curves in figure 9 show the time dependences of the nuclear exciton decay for a thick target $\mu_n z = 21.5$ for the same values of jump rate. When diffusion is small,

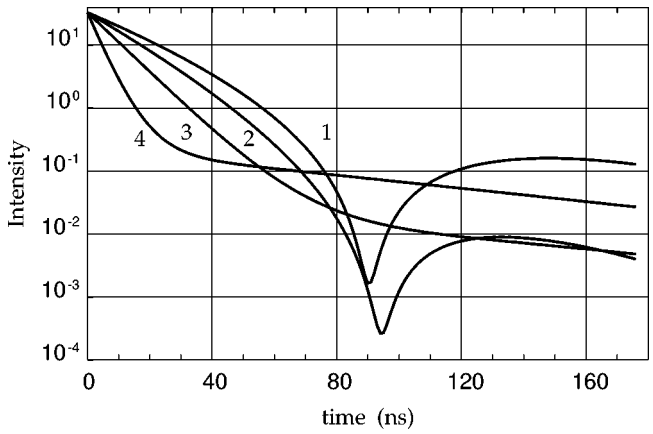

Figure 9. Time spectra of forward scattering for jump diffusion in a thick target.

the relevant curves contain dynamical beat minima characteristic for scattering from a thick target. It is clearly seen that the positions of the beat minima are sensitive to the diffusion rate (as in the case of bounded diffusion, where it is sensitive to the cage size (see figure 7)). The observed minimum shifts towards later times with increasing diffusion coefficient. The behaviour is as if the curves correspond to different effective thicknesses of the target. With the next increase of the jump rates the dynamical minima move out of the considered time interval and the curves 3 and 4 of figure 9 become similar to curve 4 of figure 8, i.e., the target exhibits the property of a thin scatterer.

This transformation of the time dependence is related to the properties of the universal resonance function. Indeed, the splitting of the universal resonance function into several parts leads to a fragmentation of the effective resonance thickness of the target into several partial thicknesses. The contributing terms essentially determine the decay of nuclear excitons in different time intervals, in accordance with the weights and widths of Lorentzians. Roughly, the target exhibits its different partial thicknesses in different time windows. Obviously, the dynamical beat pattern should be sensitive to the change of the weights and widths of contributing Lorentzians. This is actually the physical reason for the shift of the beat minima with the change of the potential well size or of the diffusion rate.

We want to note that in the case of two contributions to a resonance, one of the natural width and the other of a strongly broadened width $q \gg 1$, an approximate analytical description can be obtained, namely, when $t \ll t_0/q$,

$$I_{\mathrm{FS}}(t,z) \approx \frac{8}{9} C_z \exp\left(-q\frac{t}{t_0}\right) \frac{4\mathrm{J}_1^2(\sqrt{8\mu_n z t/9t_0})}{\mu_n z t/t_0}, \tag{6.9}$$

where C_z is determined by eq. (3.5). The formula claims that the decay in the initial time interval is completely determined by the broadened component of the resonance. In this time interval the evolution of the forward scattered intensity is similar to the

case of free diffusion and via parameter q one can determine the diffusion coefficient $D = a^2/32\tau$.

At later times the decay is determined by the narrow component, namely, when $t \gg t_0/q$,

$$I_{\mathrm{FS}}(t,z) \approx \frac{1}{9} C_z \exp\left(-\mu_n \frac{8z}{9q} - \frac{t}{t_0}\right) \frac{4\mathrm{J}_1^2(\sqrt{\mu_n z t/9t_0})}{\mu_n z t/t_0}. \tag{6.10}$$

The latter formula shows an interesting property of the time spectrum of nuclear resonant scattering affected by diffusion. After the characteristic time $t_c = t_0/q$ the decay of a nuclear exciton goes as without diffusion but with changed parameters. First of all, the effective thickness of the target becomes smaller according to the weight of the unbroadened component. This makes the decay slower. On the other hand, the presence of a widened component leads to a constant factor which plays the role of additional absorption, like an electronic absorption with effective thickness $8z/9q$.

The same property is also found for bounded diffusion at large enough delay time. We note that the characteristic time t_{c}, which divides the intervals of different behaviour, does not depend on the target thickness. One can see this property by comparing curves 3 and 4 in figures 8 and 9.

Finally, we note that the considerations presented above deal with the pure diffusion process, while the relaxation process is assumed to be the same as without diffusion.

7. Conclusion

The response of a nuclear ensemble in the presence of a diffusive motion of nuclei is described by the universal resonance function $\varphi(\mathbf{k},\omega)$ which is related to the Van Hove space–time correlation function $G(\mathbf{r},t)$. While considering a scattering problem, it is natural to use the momentum–time correlation function $F(\mathbf{k},t)$ which enters directly into the time dependence of nuclear exciton decay in the limit of a thin target for either regime of diffusion. The spectral density of this function $F(\mathbf{k},\omega)$ is found by the Fourier transform of $F(\mathbf{k},t)$. Actually, the universal resonance function $\varphi(\mathbf{k},\omega)$ represents the averaging of the standard resonance amplitude describing the scattering process by a static nucleus over the spectral density function $F(\mathbf{k},\omega)$ which reflects, owing to the Doppler effect, the motion of particles in the nuclear ensemble.

Analytical solution for the time dependences of the coherent forward scattering of SR can be obtained only for the case of free diffusion, where the universal resonance function has a Lorentzian shape. In this case the additional width of the resonance line is simply proportional to the diffusion coefficient. An additional exponential factor appears in the time response, the decrement of which contains the diffusion coefficient. This yields an accelerated decay of the coherent signal. The dynamical beat structure does not depend on the resonance broadening.

In contrast to the regime of free diffusion, in the case of bounded diffusion in a potential well and in the case of jump diffusion between the potential wells

(vacancies in solids) the universal resonance function has a more complicated shape, represented in general by the coherent superposition of the Lorentzian functions, where the weight and the width of a separate Lorentzian are determined by the specific character of the diffusion process. The main physical parameters affecting the shape of the universal function are the diffusion coefficient, the temperature and the parameters of the potential profile or the jump rates.

Such a shape of the universal function corresponds to a more complicated behaviour of the time response. In general, there are several stages of the decay, which are characterized by the different decay rates and the time dependence. The initial stage reveals a faster monotonous decay that is the more accelerated, the larger the diffusion coefficient and the size of the potential well are. At later times the decay rate is slowing down and the dynamical beats appear in the case of a thick target. The dynamical beat pattern is changed drastically (in contrast to the free diffusion regime) depending either on the size of the potential well in the case of bounded diffusion or on the temperature in the case of jump diffusion. When both parameters are increasing, a transition to a beat pattern characteristic for a thinner target occurs. The physical reason of this result lies in the splitting of the universal resonance function into several terms. It leads to a fragmentation of the effective resonant thickness of the target into relevant partial thicknesses. When the contributing Lorentzians have essentially different widths, the target exhibits its partial thicknesses in the time dependence of forward scattering within different time intervals. Hence, a time-variable thickness is characteristic for the nuclear exciton decay in these cases rather than a unique thickness. In general, the effect of thickness splitting is revealed for an arbitrary relation between the weights and widths of contributing Lorentzians. The dynamical beat pattern is sensitive to this relationship. However, under conditions close to the free diffusion regime, i.e., for a well size large compared to the wavelength of the radiation in the case of bounded diffusion or for high temperatures in the case of jump diffusion, the dynamical beat pattern characteristic for the full effective thickness of the target is restored.

The time evolution of the coherent forward scattering of synchrotron radiation is thus transformed not only quantitatively but also qualitatively in contrast to the relevant Mössbauer spectra. This higher sensitivity of the measurements occurs because an interference technique (forward scattering) reveals complex amplitudes of oscillations of the electromagnetic field while a spectroscopic method (resonance absorption) exhibits only their strengths. This makes forward scattering of synchrotron radiation a method with great perspectives for the study of diffusion.

References

[1] G.V. Smirnov and V.G. Kohn, Phys. Rev. B 52 (1995) 3356.
[2] L. Van Hove, Phys. Rev. 95 (1954) 249.
[3] K.S. Singwi and A. Sjölander, Phys. Rev. 120 (1960) 1093.
[4] A.M. Afanasev and V.E. Sedov, Phys. Status Solidi B 131 (1985) 299.

[5] T. Chudley and R.J. Elliott, Proc. Phys. Soc. 77 (1961) 353.
[6] M.A. Krivoglaz, Zh. Èksper. Teoret. Fiz. 40 (1961) 1812.
[7] J.M. Rowe, K. Sköld, H.E. Flotow and J.J. Rush, J. Phys. Chem. Solids 32 (1971) 41.
[8] M.A. Krivoglaz and S.P. Repetskii, Fiz. Tverd. Tela (Leningrad) 8 (1966) 2908, or see Soviet Phys. Solid State 8 (1967) 2325; Fiz. Met. Mettaloved. 32 (1971) 899, or see Soviet Phys. Met. Mettalorg. 32 (1971) 1.
[9] W. Petry and G. Fogl, Z. Phys. B – Condens. Matter 45 (1982) 207.
[10] I. Nowik, E.R. Bauminger, S.G. Cohen and S. Ofer, Phys. Rev. A 31 (1985) 2291.
[11] W. Nadler and K. Schulten, Phys. Rev. Lett. 51 (1983) 1712.
[12] O.G. Randl, B. Sepiol, G. Vogl, R. Feldwisch and K. Schroeder, Phys. Rev. B 49 (1994) 8768.
[13] E. Gerdau, R. Rüffer, H. Winkler, W. Tolksdorf, C.P. Klages and P. Hannon, Phys. Rev. Lett. 54 (1985) 835.
[14] J.B. Hastings, D.P. Siddons, U. van Bürck, R. Hollatz and U. Bergmann, Phys. Rev. Lett. 66 (1991) 770.
[15] Y. Kagan, A.M. Afanasev and V.G. Kohn, J. Phys. C 12 (1979) 615.
[16] V.G. Kohn and G.V. Smirnov, Phys. Rev. B 57 (1998) 5788.
[17] F. Volino and A.J. Dianoux, Mol. Phys. 41 (1980) 271.
[18] B. Sepiol, A. Meyer, G. Vogl, R. Rüffer, A.I. Chumakov and A.Q.R. Baron, Phys. Rev. Lett. 76 (1996) 3220.
[19] B. Sepiol, A. Meyer, V.G. Kohn, R.Rüffer, H. Franz and G. Vogl, in: *Defect and Diffusion Forum*, Vols. 143–147 (1997) p. 1311.